

# Adversarial Noise Layer: Regularize Neural Network By Adding Noise

Zhonghui You<sup>†</sup>, Jinmian Ye<sup>‡</sup>, Kunming Li<sup>§</sup>, Zenglin Xu<sup>‡</sup>, Ping Wang<sup>†</sup>

<sup>†</sup>School of Electronics Engineering and Computer Science, Peking University

<sup>‡</sup>University of Electronic Science and Technology of China

<sup>§</sup>Australian National University

zhonghui@pku.edu.cn, jinmian.y@gmail.com, u5580030@anu.edu.au

zenglin@gmail.com, pwang@pku.edu.cn

## Abstract

In this paper, we introduce a novel regularization method called Adversarial Noise Layer (ANL) and its efficient version called Class Adversarial Noise Layer (CANL), which are able to significantly improve CNN's generalization ability by adding carefully crafted noise into the intermediate layer activations. ANL and CANL can be easily implemented and integrated with most of the mainstream CNN-based models. We compared the effects of the different types of noise and visually demonstrate that our proposed adversarial noise instruct CNN models to learn to extract cleaner feature maps, which further reduce the risk of over-fitting. We also conclude that models trained with ANL or CANL are more robust to the adversarial examples generated by FGSM than the traditional adversarial training approaches.

Although Convolutional Neural Networks (CNNs) are powerful and widely used in various computer vision tasks, they suffer from over-fitting due to the excessive amount of parameters (Srivastava et al. 2014). The initial development of the neural network was inspired by the mechanism of human brain (Rosenblatt 1957) which does not work as precisely as the computer. Inspired by the difference, we infer that adding noise into the process of training could instruct CNNs to learn more robust feature representations to against the effect of noise, thereby reducing the risk of over-fitting.

Many regularization methods (Zhong et al. 2017; Simonyan and Zisserman 2015; Krizhevsky, Sutskever, and Hinton 2012) have been proposed to prevent over-fitting by adding noise into the training data. Besides, methods like DisturbLabel (Xie et al. 2016) randomly changed the label of a small subset of samples to incorrect value each iteration, thereby regularizing the CNNs on loss layer.

Sankaranarayanan et al. proposed a regularization method called Layerwise Adversarial Training (LAT) (Sankaranarayanan et al. 2018) which uses the gradients of the previous batch to generate noise for the current batch during training. Different from data augment methods, LAT adds the perturbations not only to the input images, but also the intermediate layer activations.

In this work, we propose a variant of LAT and its efficient version, we call them Adversarial Noise Layer (ANL) and Class Adversarial Noise Layer (CANL) respectively. Unlike LAT, ANL generates the noise base on the current batch gradients. CANL further reduces additional time costs by

caching the gradients based on image category.

ANL and CANL are well compatible with various CNN architectures and can be injected without changing the design philosophy. ANL and CANL are only embedded in the model during the training, so that it actually takes no extra computation in the inference process. Our main contributions are summarized as follows:

- We introduce a CNN regularization method called ANL. The empirical results show that ANL can significantly improve the performance of various mainstream deep convolution neural networks on popular datasets (Fashion-MNIST, CIFAR-10, CIFAR-100, ImageNet).
- We introduce the CANL algorithm, which is an efficient version of ANL. Compared to ANL, CANL takes less training time, but at the cost of slight degeneration in regularization performance.
- We demonstrate that ANL and CANL provide stronger regularization compared to LAT and Dropout. We also verified that ANL and CANL can improve the robustness of the CNN models, comparable to the traditional adversarial training approach, under the attack of Fast Gradient Sign Method (Goodfellow, Shlens, and Szegedy 2015).

## Related Work

The recent rapid progress of CNNs in computer vision tasks such as image classification, semantic segmentation (He et al. 2017) and image restoration (Qian et al. 2017) is partly due to the creation of large-scale dataset such as ImageNet (Russakovsky et al. 2015b) *etc.* It is commonly believed that robust models usually require large-scale sufficient training data set or expensive computation to avoid over-fitting (Lee et al. 2015). Therefore, to overcome the over-fitting challenge, various methods and techniques are proposed such as optimization techniques (Srivastava et al. 2014), regularization methods and *etc.*

The early solutions for avoiding over-fitting is to constrain the parameters by using the  $\ell_2$  regularization (Krizhevsky and Hinton 2009) or to stop training before convergence. Various regularization methods aim to reduce over-fitting are proposed recently. With a certain probability, the dropout method reduces over-fitting in large feed-forward neural networks by masking a random subset of the hidden neurons

with zero during training (Srivastava et al. 2014) but performs unsatisfactorily in tiny or compact networks. Drop-Connect (Wan et al. 2013) randomly masks the weights with zero in training phase. Stochastic Pooling (Zeiler and Fergus 2013) changes the deterministic pooling operation with randomly selects activations according to a certain distribution during training.

Recently, regularization methods by adding noise are introduced (Krizhevsky, Sutskever, and Hinton 2012; Simonyan and Zisserman 2015; Zhong et al. 2017). Simonyan et al. (Simonyan and Zisserman 2015) introduced the methods to avoid over-fitting by random horizontal flipping train data, which directly enlarge the training dataset. Zhong et al. (Zhong et al. 2017) and Krizhevsky et al. (Krizhevsky, Sutskever, and Hinton 2012) further proposed data augmentation methods through erasing training and crop training dataset randomly. Adversarial Training (Goodfellow, Shlens, and Szegedy 2015) enlarged training data set by adding adversarial training data to reduce the model sensitivity and improve the robustness of CNN models. DisturbLabel (Xie et al. 2016) added noise at the loss layer through randomly changing the label of a small subset of samples to incorrect values during training, thereby regularizing the CNN models.

Different from the methods mentioned above, our approaches regularizes CNN models by adding adversarial noise in hidden layers, learning more robust feature representations. ANL can be integrated easily into the most CNN-based models and obtain better performance.

## Method

### Terminology and Notation

To simplify, in this paper we use the following notations and terminologies to illustrate our algorithm:

- $J(\mathbf{x}, y; \theta)$  denotes the cost function used to train the model, where  $\mathbf{x}$  denotes the input image,  $y$  denotes the corresponding true label, and  $\theta$  denotes the parameters of the model.
- $\mathbf{h}_t$  denotes the output of  $t^{th}$  layer of the neural network.
- $s(\mathbf{h}_t)$  is the standard deviation of  $\mathbf{h}_t$ .
- $\boldsymbol{\eta}_t$  is the adversarial noise for  $\mathbf{h}_t$ . Suppose the network has  $L$  layers, and we treat the input as the  $0^{th}$  layer,  $\boldsymbol{\eta} = (\boldsymbol{\eta}_0, \boldsymbol{\eta}_1, \boldsymbol{\eta}_2, \dots, \boldsymbol{\eta}_L)^T$  denotes the entirety of the adversarial noise.
- $\epsilon$  is the hyper-parameter used to control the magnitude of the noise for ANL and CANL.
- $Clip_{<a,b>}(v)$  denotes the element-wise clipping  $v$ , with  $v_i$  clipped to the range  $[a, b]$ .
- $\mathcal{N}(\mu, \sigma^2)$  denotes the Gaussian distribution where  $\mu$  is the mean and  $\sigma$  is the standard deviation (std).

### Adversarial Noise Layer

The minimum distance to the decision boundary, which is regarded as the notation of margin, plays a foundational role in several profound theories and has empirically contributed

to the overwhelming performance of both classification and regression tasks (Vapnik 1995). It is commonly believed that a robust image classification model has a large margin. Take linear classifier into consideration, the direction of gradient vector  $\nabla_{\mathbf{x}} J(\mathbf{x}, y)$  vertically points to the decision boundary, meaning that  $\hat{\mathbf{x}} = \mathbf{x} + \epsilon \nabla_{\mathbf{x}} J(\mathbf{x})$  is more close to the decision boundary than  $\mathbf{x}$ .

Taking  $\hat{\mathbf{x}}$  to train will lead to higher cross-entropy loss and push the decision boundary away from  $\mathbf{x}$  more significantly, which contributes to producing a larger margin classifier (Goodfellow, Shlens, and Szegedy 2015).

Similarly, we apply this idea to CNNs. The modern view of deep CNN architectures is that deep neural network extracts the vision features layer by layer (Zeiler and Fergus 2014). We use  $\mathbf{h}_t$  to represent the output of  $t^{th}$  layer; denote the sub-network from the first layer to the  $t^{th}$  layer as  $N_t^-$ ; denote the sub-network from  $(t+1)^{th}$  layer to the last layer as  $N_t^+$ .  $\mathbf{h}_t$  is the output of  $N_t^-$  and the input of  $N_t^+$ .

Adding the specific perturbation  $\epsilon \nabla_{\mathbf{h}_t} J$  to  $\mathbf{h}_t$  leads to higher cross-entropy loss for  $N_t^+$ , which is also the loss for the whole network  $N$ . Although it is difficult to figure out the rigorous mathematical proofs on deep neural network, we conjecture that to reduce the loss, two changes will be conducted by the back-propagation update. For the sub-network  $N_t^+$  which takes the  $\mathbf{h}_t$  as input, the update tends to push the boundary away from  $\mathbf{h}_t$ . For the sub-network  $N_t^-$  which generates  $\mathbf{h}_t$  as output, the update tends to push the  $\mathbf{h}_t$  away from the boundary. As result, the perturbation  $\epsilon \nabla_{\mathbf{h}_t} J$  instructs  $N_t^+$  to learn a larger margin classifier; instructs  $N_t^-$  to extract more distinctive features  $\mathbf{h}_t$  for different class  $\mathbf{x}$  (Figure 3). Considering these assumptions, we further propose Adversarial Noise Layer (ANL). ANL simply adds the adversarial noise  $\boldsymbol{\eta}_t$  to  $\mathbf{h}_t$  using Eq. (1) and pass  $\hat{\mathbf{h}}_t$  to the next layer in the process of training.

$$\hat{\mathbf{h}}_t = \mathbf{h}_t + \boldsymbol{\eta}_t \quad (1)$$

The noise is only added during training. After the training ends, the noise layers will be wipe out and  $\hat{\mathbf{h}}_t$  will be set as  $\mathbf{h}_t$  in the inference phase. Therefore, ANL actually takes no extra computation in inference. According to the assumptions above, the adversarial noise  $\boldsymbol{\eta}_t$  is designed on the basis of the gradient of  $\mathbf{h}_t$  (Eq. 4).

$$r = Clip_{<0,\epsilon>} \left\{ \mathcal{N} \left( \frac{\epsilon}{2}, \left( \frac{\epsilon}{4} \right)^2 \right) \right\} \quad (2)$$

$$\mathbf{g}_t = \nabla_{\mathbf{h}_t} J(\mathbf{x}, y; \theta, \boldsymbol{\eta})|_{\boldsymbol{\eta}=0} \quad (3)$$

$$\boldsymbol{\eta}_t = r s(\mathbf{h}_t) \frac{\mathbf{g}_t}{\|\mathbf{g}_t\|_{\infty}} \quad (4)$$

The random scalar  $r$  is used to control the magnitude of the noise. We found that CNN models trained with dynamic magnitude noise achieve better performance than the models trained with fixed magnitude. We also multiply  $r$  by  $s(\mathbf{h}_t)$  for the intuition that the layer with a wide range of activations could tolerate relatively large perturbation. We verified the validity of  $s(\mathbf{h}_t)$  in Experiments section.

Training with ANL requires an additional forward and backward propagation to generate the adversarial noise. We name this process as the two-rounds-training strategy which

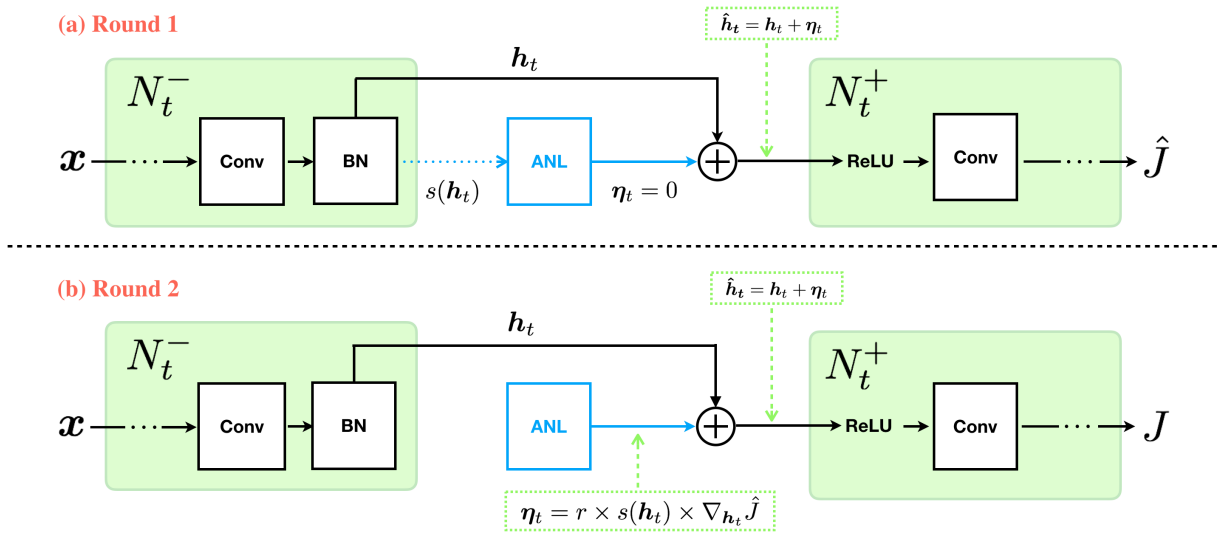


Figure 1: An illustration of two-rounds-training strategy that used by ANL. In the first round (a), ANL calculates  $s(\mathbf{h}_t)$  in forward phase and  $\nabla_{\mathbf{h}_t} \hat{J}$  in backward phase. In the second round (b), ANL will generate noise in accordance with  $s(\mathbf{h}_t)$  and  $\nabla_{\mathbf{h}_t} \hat{J}$ , then the parameters of the network will be updated by back-propagation. For CANL, only one round of training is required because the gradients come from the cache.

is shown in Figure 1. As the figure shows, adversarial noise is calculated after the first back-propagation and network is updated after the second back-propagation (Algorithm 1).

---

#### Algorithm 1 Training with ANL

---

**Require:**  $\epsilon > 0$

**repeat**

Sample a batch  $\{\mathbf{X}, \mathbf{Y}\}$  from the training data.  
 Forward-propagation calculate the loss  $J(\mathbf{X}, \mathbf{Y}; \theta, 0)$   
 and standard deviation of intermediate activations.  
 Backward-propagation calculate the gradients.

**for**  $t := 1$  to  $L$  **do**

update  $\eta_t$  with Eq. (4)

**end for**

Second forward-propagation get  $J(\mathbf{X}, \mathbf{Y}; \theta, \eta)$   
 Second backward-propagation calculate the gradients.  
 Update network with  $\theta \leftarrow \theta - \lambda \nabla_{\theta} J(\mathbf{x}, \mathbf{y}; \theta, \eta)$

**until** training finish

---

### Class Adversarial Noise Layer

The two-rounds-training strategy almost doubles the training time, which is the main drawback of ANL. To reduce the extra time cost, we further proposed Class Adversarial Noise Layer (CANL) that caches gradients according to the sample category and use it for the next batch training. The noise calculation of CANL is similar to ANL’s formula Eq. (4). The difference is that CANL obtains  $\mathbf{g}_t$  from the cached gradients according to the class of the current sample. Please refer to Algorithm 2 for more details.

The reason why we cache gradients by class is that the gradients generated by the same class of samples are much

class $c$	0	1	2	3	4
$\varphi$	0.77	0.07	-0.13	0.09	0.03
class $c$	5	6	7	8	9
$\varphi$	-0.10	-0.12	0.05	-0.08	0.02

Table 1: The average of gradient similarity between samples from class 0 and samples from class  $c$ . It should be noted that we first normalize the gradients using the maximum norm, and then calculate the similarity by Eq. (5).

more similar. We trained a LeNet-5 (LeCun et al. 1998) network on MNIST for 3 epochs. Table 1 shows the average of the gradient similarity between samples from class 0 and samples from other classes. The similarity is calculated by Eq. (5). As shown in Table 1, different samples from the same class produced the gradients that were much more similar than the gradients of samples from different classes.

$$\varphi(\mathbf{g}_a, \mathbf{g}_b) = \frac{\mathbf{g}_a \cdot \mathbf{g}_b}{\|\mathbf{g}_a\|_2 \cdot \|\mathbf{g}_b\|_2} \quad (5)$$

### Compare to LAT

Both LAT and our approaches provide regularization by perturbing the intermediate layer activations. LAT calculates the perturbation by Eq. (7).

$$\mathbf{g}_t^b = \nabla_{\mathbf{h}_t} J(\mathbf{x}, \mathbf{y}; \theta, \hat{\eta}_t^b) \quad (6)$$

$$\hat{\eta}_t^{b+1} = \epsilon \text{sign}(\mathbf{g}_t^b) \quad (7)$$

$\mathbf{g}_t^b$  is the gradients of the  $t^{\text{th}}$  layer, calculated by back-propagation when the model takes the batch  $b$  samples as input. LAT simply stores the gradients from previous batch training and use them for the current batch training noise.

---

**Algorithm 2** Training with CANL

---

**Require:**  $\epsilon > 0$  $G_t^c$  is the  $t^{\text{th}}$  layer gradient cache for class  $c$ . The network containing  $L$  convolutional blocks. Training data containing  $C$  classes.**for**  $t := 1$  to  $L$  **do****for**  $c := 1$  to  $C$  **do** $G_t^c \leftarrow 0$ **end for****end for****repeat**Sample a batch  $\{X, Y\}$  from the training data.**for**  $t := 1$  to  $L$  **do**Get gradients  $g_t$  from the cache  $G_t$  according to  $Y$  to calculate noise  $\eta_t$ .**end for**Forward-propagation calculate the loss  $J(X, Y; \theta, \eta)$ 

Backward-propagation calculate the gradients.

**for**  $t := 1$  to  $L$  **do**For every class  $c$  in  $Y$ , we random sample a corresponding  $x$  from  $X$  and then update cache with $G_t^c \leftarrow \nabla_{h_t} J(x, y; \theta, \eta)$ .**end for**Update network with  $\theta \leftarrow \theta - \lambda \nabla_{\theta} J(X, Y; \theta, \eta)$ **until** training finish

---

$\hat{\eta}_t^{b+1}$  is the noise calculated base on  $g_t^b$ , and it will be added to the activations of  $t^{\text{th}}$  layer during the batch  $b+1$  training. LAT and our approaches differ in the following ways:

- LAT uses the gradients from the previous batch to generate perturbations for the activations of the current batch. Since the gradients similarity between different classes is relatively low, there is no guarantee that the noise calculated by LAT will always increase the loss, which limits the regularization performance of LAT. Unlike LAT, ANL adopts the gradients from the current batch to ensure the effectiveness of the noise. On the other hand, CANL takes advantage of the cached gradients from the same class samples. We demonstrate, in Experiments section, that ANL and CANL have achieved better results than LAT in our tests.
- We regulate noise according to the standard deviation of the layer activations. We verify the validity of standard deviation in the Experiments section. Other minor improvements have also been adopted, including random magnitude and maximum norm (Eq. 4).

## Experiments

We first conduct a qualitative study on ANL and CANL by analyzing the influence of different noise on the feature maps. Then, we demonstrate the high compatibility of ANL and CANL by carrying out experiments in various mainstream CNN architectures. In the end, we validated the robustness of the models trained with ANL and CANL to the adversarial samples generated by FGSM.

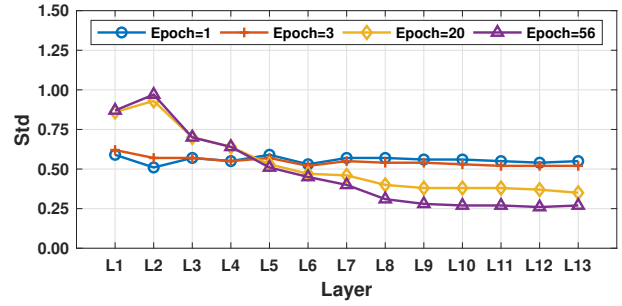


Figure 2: The standard deviation of the activation of layers under different epoch.

## The Impact of Various Noise

It is a straightforward way to visually illustrate the impact of adversarial noise by analyzing the feature maps calculated by the convolutional layers. We conducted the experiments with the LeNet-5 (LeCun et al. 1998)<sup>1</sup> network on Fashion-MNIST (Xiao, Rasul, and Vollgraf 2017) dataset.

Firstly, under the same initialization conditions, we trained five LeNet-5 models with different types of noise on the Fashion-MNIST dataset. Then we wipe out all of the noise layers and extract the output of the first convolution layer, and put them through a sigmoid function to get the feature maps.

Figure 3 shows the feature maps while the input was sampled from the test dataset. Compared with the baseline, it is observed that the Gaussian noise make little difference while adversarial noise has an apparent impact on feature extraction for the network. In addition, the feature maps from the model trained with adversarial noise have sharper skeleton and structure, which indicates the model trained with adversarial noise tends to extract more distinct features for different class images. CANL shows the similar effects to ANL. It has also been found that adding the noise opposite to adversarial noise, *i.e.*, setting negative  $\epsilon$ , tends to severely blur the feature maps, which leads to a tremendous score drop in our test. This is in line with our expectations, because according to the assumptions we discussed in the Methods section, noise that is opposite to adversarial noise might shorten the margin distance.

The quantitative comparison is shown in Table 2. We also explore the effects of different noises on the VGG-16 (Simonyan and Zisserman 2015) and ResNet (He et al. 2016a) models using CIFAR-10 and CIFAR-100 (Krizhevsky and Hinton 2009) datasets. The models are initialized with the same random seed. We follow the experiments setting employed in (Sankaranarayanan et al. 2018): We use the SGD solver with Nesterov momentum of 0.9. The learning rate started at 0.1 and it is dropped by 5 every 50 epochs. All models are trained for 300 epochs. We also randomly perform horizontal flips and take a random crop with size 32x32 from images padded by 4 pixels on each side for the CIFAR-10 and CIFAR-100 experiments.

<sup>1</sup>CONV-ANL-RELU-POOL-CONV-ANL-RELU-POOL-FC-RELU-FC-RELU-FC

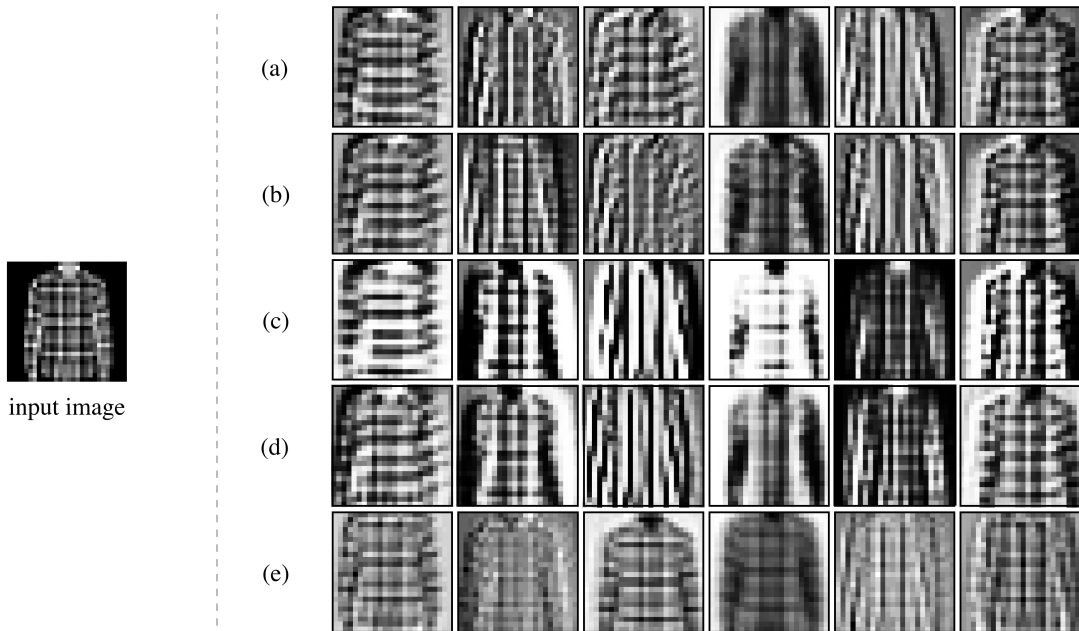


Figure 3: An illustration of feature maps from LeNet-5 (LeCun et al. 1998) models trained with different noise. Each row represents the feature maps of all 6 channels of the first convolutional layer. The left is the input image. (a) is the feature maps from the baseline network which is trained without noise. (b) is from the network trained with the Gaussian noise from  $\mathcal{N}(0, (\epsilon/4)^2)$  where  $\epsilon = 0.03$ . (c) is from the network trained with ANL where  $\epsilon = 0.03$ . (d) is from the network trained with CANL where  $\epsilon = 0.03$ . (e) is from the network trained with ANL where  $\epsilon = -0.03$ .

Model	Dataset	Baseline	Gaussian	LAT	ANL $\epsilon = 0.03$	ANL $\epsilon = -0.03$	CANL $\epsilon = 0.03$
Lenet-5	Fashion-MNIST	9.44	9.49	-	<b>8.87</b>	12.00	9.21
VGG-16	CIFAR-10	7.81	7.92	7.35	<b>6.19</b>	54.31	6.32
ResNet-20	CIFAR-10	9.71	9.88	8.90	<b>7.14</b>	74.06	7.45
ResNet-56	CIFAR-10	8.45	8.54	5.90	<b>5.35</b>	75.80	5.46
ResNet-20	CIFAR-100	36.3	37.2	33.1	<b>30.5</b>	81.27	31.9
ResNet-56	CIFAR-100	31.9	32.6	28.6	<b>27.3</b>	97.52	27.8

Table 2: The test error (%) of models trained with various noises.

As shown in Table 2, Gaussian noise slightly reduced the accuracy of the model. LAT, ANL and CANL all show regularization capabilities and achieve better accuracy than the baseline. Compared with the other regularization methods, ANL achieves the best results. CANL is slightly inferior to ANL, but significantly better than LAT. In addition, we notice that the VGG-16 model achieved 99.6% accuracy on the CIFAR-10 training set after few epochs of training using the ANLs that configured with negative  $\epsilon$ , but the accuracy on test set is not higher than 45.69%. For the ResNet models, the degeneration is even significant. We infer that the noise opposite to the adversarial noise will result in a significant reduction in model’s accuracy because the model is unable to extract distinct features.

We implement ANL and CANL base on the Pytorch framework and ran experiments on the Titan Xp GPUs. The average time to train the VGG-16 baseline model on CIFAR-10 for one epoch was 14.26 seconds. The model that integrated with ANL cost 27.57 seconds to train for one epoch,

while CANL took 15.83 seconds which is very close to the baseline. In general, CANL has achieved a good tradeoff between training cost and regularization capability.

#### Further research on ANL and CANL capabilities

We first verify the validity of the standard deviation in Eq. (4). Then we investigate the effect of the hyperparameter  $\epsilon$ . Further, we demonstrate that ANL and CANL can be integrated with most of the mainstream CNN architectures and compared them with Dropout. Lastly, we conduct experiment on ImageNet to demonstrate the regularization capabilities of ANL and CANL on large-scale data set.

**Validity of the standard deviation** We first train a VGG-16 network integrated with ANL on CIFAR-10, of which the adversarial noise was calculated without  $s(h_t)$ . Figure 2 shows the standard deviation of the activation of layers. As it shows, the standard deviation varies from layer to layer and changes as the model converges. The insight of using standard deviation is that if the output of the layer has a relatively

Model	$\epsilon$	Cifar10				Cifar100			
		Baseline	+Dropout	+ANL	+CANL	Baseline	+Dropout	+ANL	+CANL
MobileNet	0.02	9.25	9.88	<b>7.84</b>	7.98	34.28	34.19	<b>30.71</b>	31.16
MobileNet v2	0.02	7.83	7.86	<b>5.54</b>	5.71	29.64	30.70	<b>25.51</b>	25.93
VGG-11	0.05	8.45	8.37	<b>7.67</b>	7.79	30.47	29.97	<b>29.19</b>	29.30
VGG-16	0.05	7.47	7.16	<b>5.81</b>	5.88	29.45	28.91	<b>26.61</b>	26.73
ResNet-18	0.05	5.98	5.03	<b>4.21</b>	4.35	24.16	22.83	<b>22.23</b>	22.61
ResNet-34	0.08	5.34	4.70	<b>3.90</b>	3.97	23.42	22.14	<b>21.50</b>	21.82
PyramidNet-48	0.01	5.62	5.16	<b>4.38</b>	4.50	25.14	25.24	<b>23.33</b>	24.03
PyramidNet-270	0.10	4.68	4.10	<b>3.03</b>	3.12	19.55	18.94	<b>17.51</b>	17.94

Table 3: Test errors (%) with different architectures on CIFAR-10 and CIFAR-100 (Krizhevsky and Hinton 2009). Baseline is the model trained without noise and dropout (Srivastava et al. 2014). In (+Dropout), we insert dropout between FC layers and set drop ratio to 0.5 according to (He et al. 2016b). In (+ANL) and (+CANL), we insert noise layers after every batch normalization, and the choice of  $\epsilon$  is based on the amount of parameters of the network.

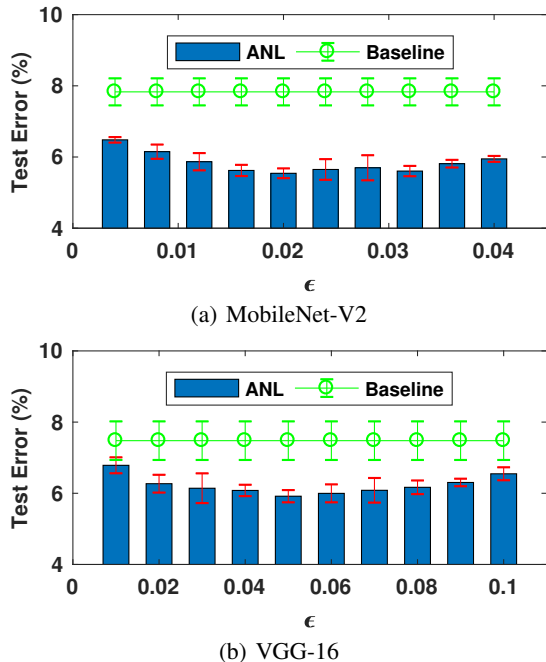


Figure 4: The test error(%) of (a) the MobileNet-V2 (Sandler et al. 2018), (b) VGG-16 (Simonyan and Zisserman 2015) on CIFAR-10, trained with ANL under different  $\epsilon$ . Results reported are average of 5 runs.

large standard deviation, it should be compatible with large perturbation. The error rate drops from 6.53% to 5.91% by taking  $s(\mathbf{h}_t)$  into account while the error rate of the baseline model that trained without noise is 7.47%.

**The choice of the hyper-parameter.**  $\epsilon$  is the only hyper-parameter required by ANL and CANL. To investigate the effect of different choices of  $\epsilon$ , we train models with two different CNN architectures on CIFAR-10 with various  $\epsilon$ . As the Figure 4 shows, each architecture has one of the most suitable choices of  $\epsilon$ . According to our experience, the network with more trainable parameters performs better on

relative big  $\epsilon$ . For example, the number of parameters of MobileNet-V2 is 2.3 million, and its best  $\epsilon$  is 0.02. The best  $\epsilon$  for VGG-16 (14.7 million) is about 0.05, while the best  $\epsilon$  for ResNet-18, which has around 11.2 million trainable parameters, is also close to 0.05. But it is not always the case, because the optimal value of  $\epsilon$  is also affected by the model architecture.

**Integrate with various CNN architectures** To show the compatibility of ANL and CANL in various architectures, we train various models with and without the noise layers on the CIFAR-10 and the CIFAR-100 dataset. Five architectures are adopted: MobileNet (Howard et al. 2017), MobileNet v2 (Sandler et al. 2018), VGG (Simonyan and Zisserman 2015), ResNet (He et al. 2016a) and PyramidNet (Han, Kim, and Kim 2017). We also compared the proposed algorithms with dropout.

The learning rate started at 0.1 and would be divided by 2 unless the last 5 epoch validation loss reaches lower value than the best ever seen. Each learning rate stays at least 5 epoch and the minimum learning rate is 0.001. We use a weight decay of  $5e-4$  and momentum of 0.9 for all experiments. We train the baseline for 200 epoch. In comparison, the network is trained with ANL and CANL for the first 100 epoch. Then we disable the noise layers and set the learning rate to the minimum (*i.e.*  $1e-3$ ) before we train the network for another 100 epoch.

The following observations can be made from Table 3. The proposed noise layer is compatible with various CNN architectures and shows a noticeable improvement from baseline. ANL had achieved the best results in all comparisons, while CANL presented very close regularization capability to ANL. For the experiments on the MobileNet model, Dropout slightly reduced accuracy, but ANL and CANL still demonstrated good regularization.

**Imagenet Experiment** In order to test the applicability of the proposed regularization methods on large-scale dataset, we conduct an experiment on the ImageNet (Russakovsky et al. 2015a) dataset. We implement AlexNet (Krizhevsky, Sutskever, and Hinton 2012) integrated with CANL, and set  $\epsilon = 0.05$ . Both the baseline and the regularized model are trained from scratch to 90 epochs. The learning rate started

$\delta$	0	2	4	6	8
Baseline	92.0	53.8	42.2	37.4	33.8
AT( $\epsilon=0.05$ )	91.9	74.5	68.8	59.7	53.9
ANL( $\epsilon=0.01$ )	92.6	67.1	57.0	52.4	47.7
ANL( $\epsilon=0.05$ )	<b>93.9</b>	<b>79.2</b>	<b>71.8</b>	<b>63.7</b>	<b>61.0</b>
CANL( $\epsilon=0.01$ )	92.6	66.9	56.3	51.0	46.3
CANL( $\epsilon=0.05$ )	93.7	75.7	65.0	58.3	55.8

Table 4: The test accuracy(%) of the VGG-16 networks on the adversarial examples that generated by FGSM with different  $\delta$ .

from 0.01 decayed by 10 every 30 epochs. The classification accuracy of the baseline is 56.35%, while the accuracy of the regularized model is 60.52%. This shows that our approaches can significantly improve the performance of deep neural networks on the large datasets like ImageNet.

### Adversarial Attack Evaluation

Deep convolutional neural networks are easily fooled by carefully designed adversarial examples. Plenty of literatures (Goodfellow, Shlens, and Szegedy 2015; Papernot et al. 2017; Kurakin, Goodfellow, and Bengio 2017; Moosavi-Dezfooli et al. 2017) show that small perturbations cause well-designed deep networks to misclassify the image easily. Although the main focus of our proposed methods is to prevent model from overfitting, we have found it is helpful in improving the robustness of the model to the adversarial examples as well.

In our experiment, we use the Fast Gradient Sign Method (FGSM) (Goodfellow, Shlens, and Szegedy 2015) to generate adversarial examples. Assuming the input image  $x$  is in the range 0 to 255, the perturbed image  $\hat{x}$  is generated as  $\hat{x} = x + \delta \text{sign}(\nabla_x J(x))$ . The value of  $\delta$  is usually set to small number relative to 255 to generate the perturbations imperceptible to human but degrade the accuracy of a network significantly.

We train six different VGG-16 networks on CIFAR-10 for the FGSM white-box attack tests. We add the noise layers not only after the convolution layers but also to the input  $x$ . The baseline model is trained without noise. For the ANL and CANL tests, we try different values of  $\epsilon$ . We also test the AT algorithm introduced by (Goodfellow, Shlens, and Szegedy 2015), which enhances the robustness of the network by using the adversarial examples for training.

The results is shown in Table 4. The value of  $\delta$  indicate the strength of the adversarial perturbation, generated by FGSM, which is added to the image to produce adversarial examples. From the table, we have the following observations: (1)  $\delta = 0$  means no adversarial perturbation is added to the images. Compared to AT, the proposed methods significantly improve the performance of the original data. (2) ANL and CANL show comparable robustness enhancements to AT (3) For ANL and CANL, a larger  $\epsilon$  increases the perturbation to the intermediate activations, providing a stronger robustness enhancement for the network.

### Conclusion

In this paper, we propose two regularization algorithms called "Adversarial Noise Layer" and "Class Adversarial Noise Layer". They are easy to implement and can be integrated with the most of CNN-based models. The proposed methods require only one hyper-parameter  $\epsilon$ , and the choice of  $\epsilon$  is related to the number of trainable parameters of the network. The noise is only added during the training process, so there is no additional computation cost for CNN models in the inference phase. Models trained with ANL or CANL have been proved to be more robust under the FGSM attack.

Currently, we only apply ANL and CANL in image classification tasks. In future work, we will explore other computer vision tasks such as object detection and face recognition. It is also interesting to explore the application of ANL and CANL in the area beyond computer vision, such as natural language processing and voice recognition.

### References

- Goodfellow, I. J.; Shlens, J.; and Szegedy, C. 2015. Explaining and harnessing adversarial examples. In *International Conference on Learning Representations (ICLR)*.
- Han, D.; Kim, J.; and Kim, J. 2017. Deep pyramidal residual networks. In *IEEE Conference on Computer Vision and Pattern Recognition (CVPR)*, 6307–6315.
- He, K.; Zhang, X.; Ren, S.; and Sun, J. 2016a. Deep residual learning for image recognition. In *IEEE Conference on Computer Vision and Pattern Recognition (CVPR)*, 770–778.
- He, K.; Zhang, X.; Ren, S.; and Sun, J. 2016b. Identity mappings in deep residual networks. In *European Conference on Computer Vision (ECCV)*, 630–645.
- He, K.; Gkioxari, G.; Dollár, P.; and Girshick, R. B. 2017. Mask R-CNN. In *International Conference on Computer Vision (ICCV)*, 2980–2988.
- Howard, A. G.; Zhu, M.; Chen, B.; Kalenichenko, D.; Wang, W.; Weyand, T.; Andreetto, M.; and Adam, H. 2017. Mobilenets: Efficient convolutional neural networks for mobile vision applications. *arXiv preprint arXiv:1704.04861*.
- Krizhevsky, A., and Hinton, G. 2009. Learning multiple layers of features from tiny images. In <https://www.cs.toronto.edu/~kriz/cifar.html>.
- Krizhevsky, A.; Sutskever, I.; and Hinton, G. E. 2012. Imagenet classification with deep convolutional neural networks. In *Conference on Neural Information Processing Systems (NIPS)*, 1106–1114.
- Kurakin, A.; Goodfellow, I.; and Bengio, S. 2017. Adversarial machine learning at scale. *International Conference on Learning Representations (ICLR)*.
- LeCun, Y.; Bottou, L.; Bengio, Y.; and Haffner, P. 1998. Gradient-based learning applied to document recognition. *Proceedings of the IEEE* 86(11):2278–2324.
- Lee, C.; Xie, S.; Gallagher, P. W.; Zhang, Z.; and Tu, Z. 2015. Deeply-supervised nets. In *Proceedings of the Eighteenth International Conference on Artificial Intelligence and Statistics (AISTATS)*, 562–570.



- Moosavi-Dezfooli, S.; Fawzi, A.; Fawzi, O.; and Frossard, P. 2017. Universal adversarial perturbations. In *IEEE Conference on Computer Vision and Pattern Recognition (CVPR)*, 86–94.
- Papernot, N.; McDaniel, P. D.; Goodfellow, I. J.; Jha, S.; Celik, Z. B.; and Swami, A. 2017. Practical black-box attacks against machine learning. In *Proceedings of the 2017 ACM on Asia Conference on Computer and Communications Security (ASIACCS)*, 506–519.
- Qian, R.; Tan, R. T.; Yang, W.; Su, J.; and Liu, J. 2017. Attentive generative adversarial network for raindrop removal from a single image. *arXiv preprint arXiv:1711.10098*.
- Rosenblatt, F. 1957. *The perceptron, a perceiving and recognizing automaton Project Para*. Cornell Aeronautical Laboratory.
- Russakovsky, O.; Deng, J.; Su, H.; Krause, J.; Satheesh, S.; Ma, S.; Huang, Z.; Karpathy, A.; Khosla, A.; Bernstein, M.; Berg, A. C.; and Fei-Fei, L. 2015a. ImageNet Large Scale Visual Recognition Challenge. *International Journal of Computer Vision (IJCV)* 115(3):211–252.
- Russakovsky, O.; Deng, J.; Su, H.; Krause, J.; Satheesh, S.; Ma, S.; Huang, Z.; Karpathy, A.; Khosla, A.; Bernstein, M. S.; Berg, A. C.; and Li, F. 2015b. Imagenet large scale visual recognition challenge. *International Journal of Computer Vision (IJCV)* 115(3):211–252.
- Sandler, M.; Howard, A.; Zhu, M.; Zhmoginov, A.; and Chen, L.-C. 2018. Inverted residuals and linear bottlenecks: Mobile networks for classification, detection and segmentation. *arXiv preprint arXiv:1801.04381*.
- Sankaranarayanan, S.; Jain, A.; Chellappa, R.; and Lim, S. 2018. Regularizing deep networks using efficient layerwise adversarial training. In *Proceedings of the Thirty-Second AAAI Conference on Artificial Intelligence*, 4008–4015. AAAI Press.
- Simonyan, K., and Zisserman, A. 2015. Very deep convolutional networks for large-scale image recognition. In *International Conference on Learning Representations (ICLR)*.
- Srivastava, N.; Hinton, G.; Krizhevsky, A.; Sutskever, I.; and Salakhutdinov, R. 2014. Dropout: A simple way to prevent neural networks from overfitting. *Journal of Machine Learning Research (JMLR)* 15(1):1929–1958.
- Vapnik, V. N. 1995. *The Nature of Statistical Learning Theory*. Springer science & business media.
- Wan, L.; Zeiler, M.; Zhang, S.; Le Cun, Y.; and Fergus, R. 2013. Regularization of neural networks using dropconnect. In *International Conference on Machine Learning (ICML)*, 1058–1066.
- Xiao, H.; Rasul, K.; and Vollgraf, R. 2017. Fashion-mnist: a novel image dataset for benchmarking machine learning algorithms. *arXiv preprint arXiv:1708.07747*.
- Xie, L.; Wang, J.; Wei, Z.; Wang, M.; and Tian, Q. 2016. Disturblabel: Regularizing cnn on the loss layer. In *IEEE Conference on Computer Vision and Pattern Recognition (CVPR)*, 4753–4762.
- Zeiler, M. D., and Fergus, R. 2013. Stochastic pooling for regularization of deep convolutional neural networks. In *International Conference on Learning Representations (ICLR)*.
- Zeiler, M. D., and Fergus, R. 2014. Visualizing and understanding convolutional networks. In *European Conference on Computer Vision (ECCV)*, 818–833.
- Zhong, Z.; Zheng, L.; Kang, G.; Li, S.; and Yang, Y. 2017. Random erasing data augmentation. *arXiv preprint arXiv:1708.04896*.